Aslı Öztürk Kiraz
Serkan Kaya
Pamukkale University, Pamukkale-Turkey
aslio@pau.edu.tr; skaya054@posta.pau.edu.tr; Pamukkale-Turkey

STRUCTURAL AND ELECTRICAL PROPERTIES OF THE $Ca(PO^-_4)_2$ COMPOUND

ABSTRACT

The use of biomaterials is increasing today and some of the most challenging materials are Calcium compounds. This computational study on calcium compound provides a framework for new materials design and selection for biomaterials used in many areas. The reason of that $Ca(PO^-_4)_2$ compound studied for this work. All the calculations are carried out on the Gaussian 09.C1 program using Density Functional Theory with the B3LYP hybrid functional method, GEN basis set (we used for phosphorus and oxygen 6-31++G(d, p), for calcium cc-pVDZ). The low HOMO-LUMO gap (1.64eV for DFT at B3LYP/GEN basis level, 0.93eV for TD-DFT at B3LYP/GEN basis level) for the molecule explains the chemical reactivity.

Keywords: Calcium Compounds, Density Functional Theory, B3LYP
            Hybrid Function, Structural Parameters,
            Electronic Properties

$Ca(PO^-_4)_2$ BİLEŞİĞİNİN YAPISAL VE ELEKRİKSEL ÖZELLİKLERİ

ÖZ

Günümüzde nano-biyomalzeme kullanımı her geçen gün artmakta ve hidroksiapatit bu alanda önemli bir yer tutmaktadır. Hidroksiapatit ile ilgili çalışmalar birçok alanda kullanılan biyomalzeme tasarımı ve seçimi için geniş bir çerçeve sunmaktadır. Bu çalışmada ise nano-hidroksiapatit yapısına benzer olarak tasarladığımız kalsiyum bileşiğinin ($Ca(PO-_4)_2$) yapısal ve elektronik parametreleri, yoğunluk fonksiyonel teorisi (YFT), etkileşim alanı B3LYP hibrid işlevsel yöntemi, GEN (fosfor ve oksijen atomları etkileşimi için 6-31++G(d,p), kalsiyum için cc–pVDZ) baz seti kullanılarak Gaussian 09.C1 paket programı ile hesaplanmıştır. Spektroskopik verileri, molekülün kimyasal olarak reaktif olduğunun göstergesi olan alçak HOMO-LUMO enerji aralığı (B3LYP/GEN temel seviyesinde DFT için) 1.64eV ve (B3LYP/GEN temel seviyesinde TD-DFT için) 0.93eV olarak elde edilmiştir.

Anahtar Kelimeler: Kalsiyum Bileşikleri, Yoğunluk Fonksiyonel
                    Teorisi, B3LYP Hibrit Fonksiyon, Yapısal
                    Parameterler, Elektronik Özellikler

1. INTRODUCTION

In the recent years there is an increasing attention to the Calcium (Ca) compounds. For this reason, in this study, we tried to investigate the $Ca(PO_4^-)_2$ compound Ca complex theoretically because $Ca(PO_4^-)_2$ compound is partially similar with hydroxyapatite (HAp) structure. Ca is the principal inorganic component of cortical bone like teeth enamel with hydroxyapatite $(Ca_5(PO_4)_3(OH))$ application [1]. Hydroxyapatite (HAp) is the naturally occurring calcium phosphate and member of apatite mineral family. HAp has been recently stood out because of its highest quality in the context of osteocompatibility and high absorbability, and has subsequently been used as a bio-material for unnatural bone [1 and 2]. HAp has been studied and used as environmentally benign functional material with adsorbent materials through changing cations or adsorbing invariable ones on the crystal surface. HAp can be derived from both synthetic and natural origins [3]. Furthermore, nano-hydroxyapatite (nano-HAp) has larger specific surface area, better mechanical properties and excellent osteoconductivity compared to conventional hydroxyapatite [4]. As a result of the fundamental function executed by HAp, $Ca(PO_4^-)_2$ compound great importance has supposed the knowledge of its structure at atomic level in addition to its lattice dynamics since this compound is similar to the HAp.

Several experimental techniques, such as X-ray diffraction [5 and 6], IR and RAMAN spectroscopy [7 and 9], NMR [10] and many others, have been performed for pure material and after mersion in simulated body fluid (SBF) so that clear up the HAp structure. However, because of the difficulties in the rendition of the experimental results and the demands of the acknowledgement of the dynamical properties of the lattice, various computational studies have also been performed and new materials have been designed, both with molecular mechanics [11 and 12] and quantum mechanical methods [13 and 14]. Recently, DFT methods are generally used to determine the molecular structures and vibrational spectra for the molecules at low computational time [15 and 24]. The experimental studies and the theoretical calculations on the structural properties of the HAp are scarcity in the literature but there is no information about $Ca(PO_4^-)_2$ compound. Clearly to understand the experimental studies, it is needed to be executed moreover the theoretical studies pointing to describe the fundamental properties of the compound DFT computations based on the quantum mechanics are generally used to study a few physical and chemical properties of the materials and chemical compounds [25 and 26].

2. RESEARCH SIGNIFICANCE

In this study, we indicated identification and molecular structure of the molecule of the $Ca(PO_4^-)_2$ compound theoretically. In addition, DFT calculations are performed for predicting the structural, vibrational, NMR, UV-Visible spectrums and electronic parameters of the $Ca(PO_4^-)_2$ compound. For adding a molecule group or atoms to the $Ca(PO_4^-)_2$ compound in the future calculations oxygens were taken into account in the reduced state.

3. MATERIALS AND METHODS

Density functional theory (DFT) and time-dependent (TD)-DFT were used to perform the quantum mechanical calculations of the Ca compound in gas phase. All the calculations were carried out with the Gaussian 09.C1 [27] package program and GaussView 5.0.9 [28] was used for the visualization of the structure and simulated vibrational

spectra.Vibrational assignments were carried out by the VEDA 4 program [29] (Vibrational EnergyDistribution Analysis). Becke3-Parameter method for calculating the part of the molecular energy due to overlapping orbitals plus the Lee-Yang-Parr method of accounting for correlation B3LYP [30] hybrid functional was employed for all DFT and TD-DFT calculations along with Pople's split-valence double-ζ 6-31++G(d,p) basis set [31 and 32] for all atoms except for calcium for which Dunning's double-ζ correlation basis set cc-pVDZ [33 and 34].

4. RESULTS AND DISCUSSION (SONUÇLAR VE TARTIŞMA)
4.1 Structural properties

This structure consists of 11 atoms and has 27 fundamental vibrational modes. The optimized structural parameters such as bond length, bond angle and dihedral angle of the title compound are presented in Table 1. The molecular structure of the title compound comprise of 10 bond lengths, 19 bond angles and 10 dihedral angles. These bond lengths, bond angles and dihedral angles are given in Table 1.

Table 1. Bond lengths and bond angles of single molecule of $Ca(PO_4^-)_2$

Bond length	(Å)	Exp. 1 [35]	Exp. 2 [36 and 37]	Exp. 3 [38]	Exp. 4 [39]	Bond angles	(°)
P1-O1	1.570	1.551	1.536	1.541	1.533	O2-P1-O3	112,73
P1-O2	1.570	1.551	1.536	1.554	1.544	O2-P1-O4	112,75
P1-O3	1.570	1.551	1.536	1.545	1.514	O2-P1-O7	105,95
P1-O7	1.580	1.551	1.536	–	–	O3-P1-O4	112,75
Ca5-O7	2.080	2.441	2.400	2.425	2.416	O3-P1-07	105,97
Ca5-O8	2.080	2.428	2.437	2.468	2.449	O4-P1-O7	105,95
P2-O8	1.580	1.551	1.536	–	–	O8-P6-O9	105,97
P2-O9	1.570	1.551	1.536	–	–	O8-P6-O10	105,95
P2-O10	1.570	1.551	1.536	–	–	O8-P6-O11	105,96
P2-O11	1.570	1.551	1.536	–	–	O9-P6-O10	112,75
						O9-P6-O11	112,73
						O10-P6-O11	112,75

Our theoretical results of the bond lengths and bond angles with the attainable corresponding experimental values given in literature. The calculated bond lengths and bond angles, as shown in Table 1, help us to realize the molecular structure of the title compound. For example, the length of the P1-O2 is measured as 1.533Å [39]. In additon to example the length of the P1-O2 is measured 1.541Å [38] while it is computed as 1.570Å by using the DFT/B3LYP levels by using with Pople's split-valence double-ζ 6-31++G(d,p) basis set, respectively. The bond angle of the O2-P1-S4 is calculated as 117.7523 by using DFT methods, respectively. The dihedral angles shown in Table 1 are coherent with each other. All the theoretical bond lengths and bond angles describing the title compound computed at B3LYP/6-31++G(d,p) level is given in Table 1. The vibrational spectroscopy analysis has been verified to be an important contributor in the study of various fields of science because of the remarkable flexibility of sampling methods. Since, the vibrational frequency analysis is one of the most useful tools for describing the chemical compounds in terms of both theoretical calculations and experimental studies. The investigation of the vibrational frequencies via ab initio computational methods is becoming spreadingly important tools in the area of chemistry. Theoretically predicted frequencies can serve one to determine the chemical compounds. In the present work, we have figured out a frequency calculation analysis to obtain the

spectroscopic value of the title compound. It includes one atom, therefore they have 27 fundamental vibrational normal modes computed by DFT method are given in Table 2, along with the assignments of fundamental vibration modes. The experimental results consistent with the theoretical results are also given in the same table. The calculated IR intensities from the DFT/B3LYP given in the table afford us to identified the fundamentals modes more exactly. That is, the calculated infrared intensity (relative intensity) determination of the strength of the transition. The computations of vibrational wavenumbers, IR intensity and the assignments of IR vibration modes of all the atoms in the compound are provided. So that, to analyze the chemical bonding in more detail, we have performed density functional theory electronic structure calculations for title compund of Ca. The narrow band in the total density of states [40] as seen Figure 1 around 8eV signifies the O 2s states followed by the 5p states of P at around 7eV and Ca at states around the 4eV with essentially no contribution from oxygen, phosphor and calcium. The bands in the energy range from 7 to 8eV originate from the PO_4^- anion (mainly O 2p mixed with In 5s states) as indicated by the MO scheme based on Extended Hückel calculations for the highest occupied states of a discrete calcium compound entity.

Table 2. TED analysis, frequency, IR and raman of the title compound

	Frequency		IR	Raman	TED Analyses
Modes	Unscaled	Scaled	Intensity	Theor.	Assignment [TED] 10 % a
1	5.75	5.52	0.0023	0.0000	δ POCa %83
2	26.16	25.14	2.0694	0.0001	τ OPOCa %67
3	27.25	26.19	2.0802	0.0001	δ OCaO %25+δ POCa %57
4	32.70	31.42	0.0001	0.6500	τ OPOCa %14+τ POCaO %70
5	33.47	32.16	0.0001	0.6509	τ OPOCa %86 + τ POCaO %13
6	91.67	88.09	91.2514	0.0002	δ OCaO %69+ δ POCa %27
7	91.74	88.16	91.2531	0.0000	τ POCaO %92
8	165.65	159.19	0.0001	10.3192	υ CaO %52 + υ PO %36
9	326.52	313.78	226.8208	0.0000	δ OPO %112
10	354.79	340.95	0.0002	1.5671	β OOOP %38
11	354.96	341.12	0.0006	1.5563	δ OPO %90
12	357.11	343.18	0.4391	0.0000	β OOOP %34
13	357.28	343.35	0.4295	0.0000	δ OPO %20+υ CaO %28+ υ PO %34
14	501.35	481.79	0.1140	0.1140	δ OPO %36
15	501.71	482.14	0.0001	0.1077	β OOOP %106
16	503.34	483.71	59.3877	0.0000	δ OPO %36
17	503.70	484.05	59.5739	0.0001	β OOOP %90
18	547.65	526.29	0.0001	36.4400	δ OPO %64+ β OOOP %20+υ CaO%13
19	568.12	545.96	101.1496	0.0001	δ OPO %32+υ CaO %18+υ PO %18
20	758.04	728.47	2160.0931	0.0000	υ CaO %35+υ PO %65
21	827.04	794.78	0.0001	24.4262	υ CaO %31+υ PO %62
22	871.24	837.26	81.8980	0.0001	υ PO %94
23	874.21	840.11	0.0001	54.4641	υ CaO %18+υ PO %72
24	985.11	946.69	0.0105	39.6601	υ PO %95
25	985.43	946.99	0.0097	39.5895	υ PO %95
26	987.05	948.55	873.6062	0.0007	υ PO %94
27	987.37	948.86	873.4318	0.0012	υ PO %94

Spectroscopic methods the main tools of modern chemistry are used to figure out and established molecular structures, to watch over the reactions and to check the purity of compounds. Most essential methods for the organic chemistry are the infrared and the Raman spectroscopy. The calculated IR intensities given in the Table 2 provide us to distinguish and assign the fundamental modes more precisely. That is, the calculated infrared intensity allows the

strength of the transition. The infrared intensities predicted at the levels of DFT for the main molecule calculated may be founded in Table 2. Note that experimental IR spectra are generally reported in either percent transmission or absorbance unit for hydroxyapatite molecules [40-42]. Explicitly, the theoretical calculations of FT-IR spectra computed from DFT/B3LYP by utilizing using with Pople's split-valence double-ζ 6-31++G(d,p) basis set of the title compound are plotted in Figure 2.
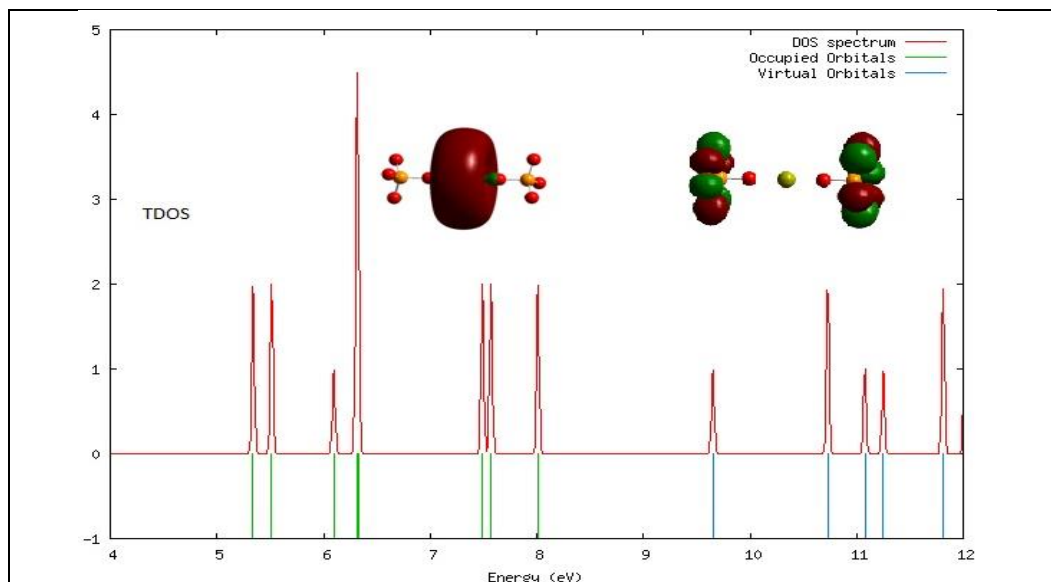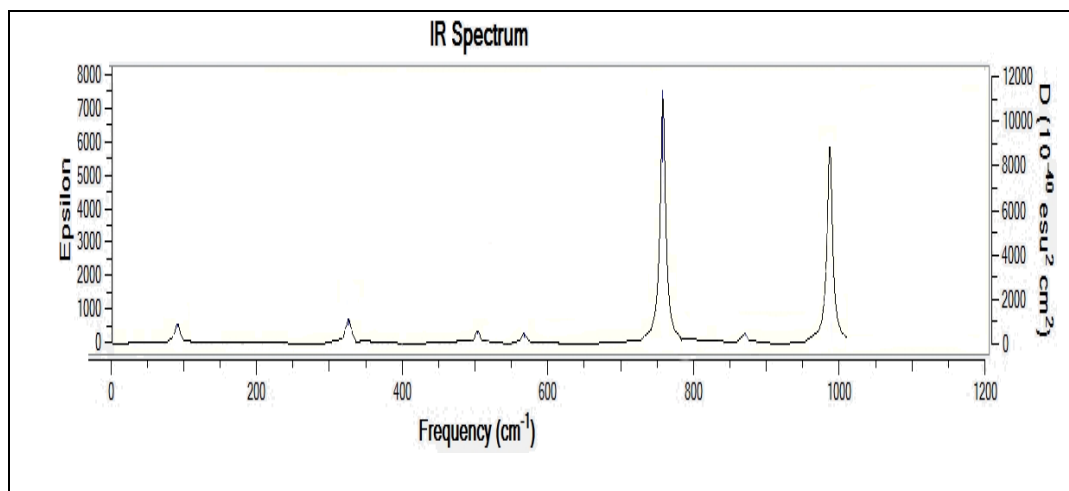

Figure 1. TDOS of calcium compound

Figure 2. Theoretical IR spectrum of the $Ca(PO_4^-)_2$

Raman Activity Spectrum

a. The Theoretical Raman spectrum of the title compound

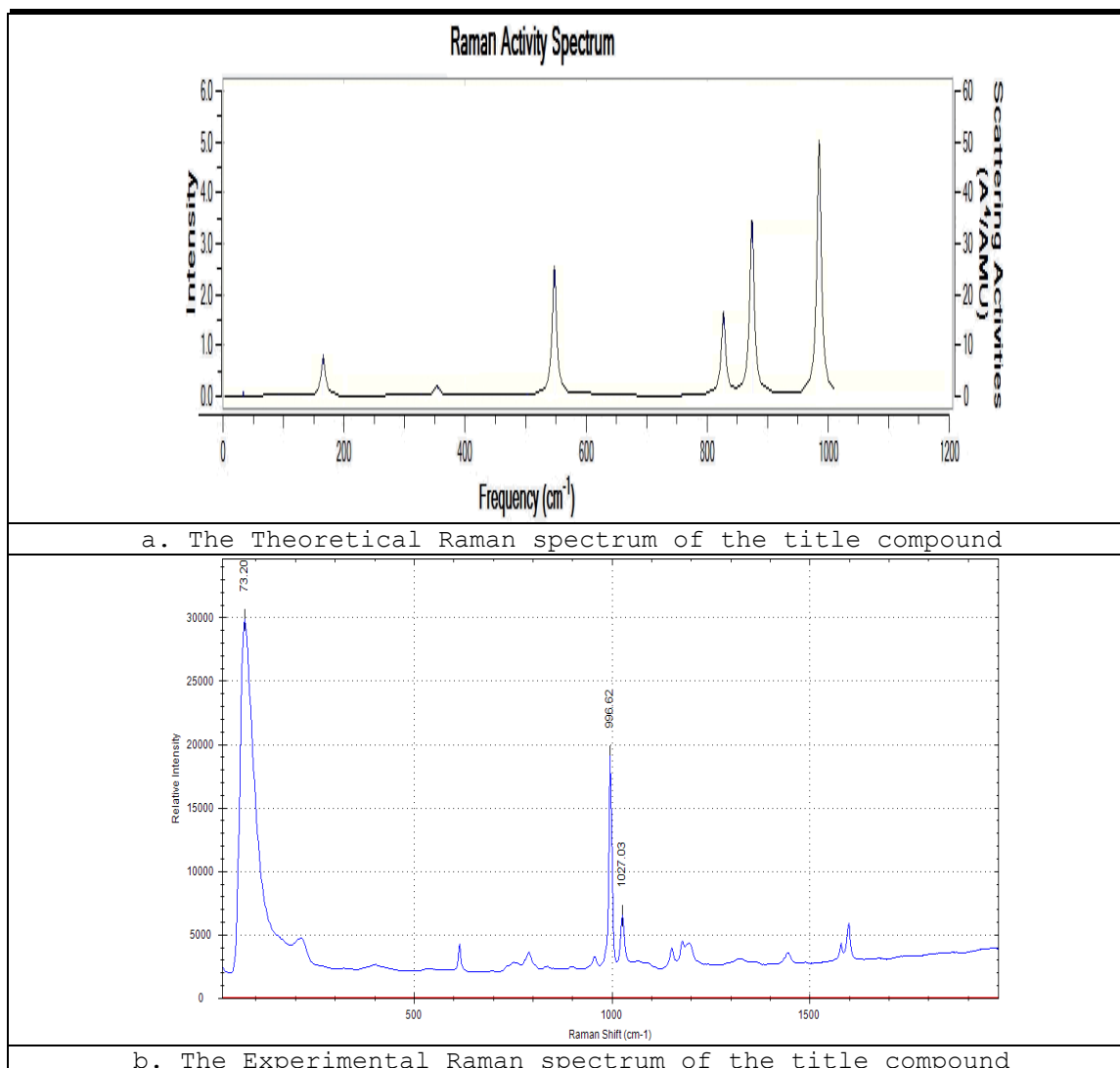b. The Experimental Raman spectrum of the title compound

Figure 3. Theoretical and Experimental Raman spectrum of the Calcium compound

The most prominent bands in the calcium compound, the Raman spectrum is from the structure, with the most intense band arising from the phosphate ν1 symmetric stretching (P-O stretching) at ~996cm^{-1}. O-O stretching at 1007cm^{-1} and Ca effects are around 500cm^{-1}. Explicitly, the Raman activities of the title compound can be seen in Figure 3 both theoretically and experimentally with Ca(PO$^{-}_4$)$_2$ compound.

4.2. Electronic Properties

HOMO and LUMO represent the ability to donate and obtain an electron [43]. The gap between HOMO-LUMO energies plays important role in the molecule chemical stability and also represents the chemical hardness-softness of the molecule, electronegativity and chemical reactivity. A molecule with small HOMO-LUMO energy gap is called a soft molecule; it is more polarizable and has high chemical reactivity and low kinetic stability, [44]. An electronic system with a larger HOMO-LUMO gap is should be less reactive than one having a smaller gap [45] also called hard molecule. As seen from the Table 3; the HOMO and LUMO energies are calculated as 8.01 and 9.65eV at the B3LYP/Gen level, 8.11 and 9.04eV at the TD-B3LYP/Gen level.

Table 3. The electronic parameters of the calcium compound

Electronic Parameters	B3LYP	TD-DFT B3LYP
E_{HOMO} (eV)	8.01	8.11
E_{LUMO} (eV)	9.65	9.04
$\Delta E = E_{LUMO} - E_{HOMO}$ (eV)	1.64	0.93
I (eV)	-8.01	-8.11
A (eV)	-9.65	-9.04
χ (eV)	-8.83	-8.58
η (eV)	0.82	0.47
σ (eV)	0.61	1.08

As seen from the Figure 4, the LUMOs are located around the Ca atom while the HOMOs are located around the P atoms. The energy gap values between HOMO and LUMO of the title compound is 1.64 and 0.93eV. These small values are the evidence of the high probability of the charge transfer in the molecule [46]. The theoretical optical properties of the biomolecules generally determine by the time-dependent density functional theory (TD-DFT) approach. The transition energies, the oscillator strengths as well as the molecular orbital (MO) compositions point out to each excited-state obtained from the TD-DFT calculations [47]. The predicting TD-DFT HOMO-LUMO gaps useful for simulation of molecular electronics and for understanding charge transfer in photoexcitation and redox chemistry [48].
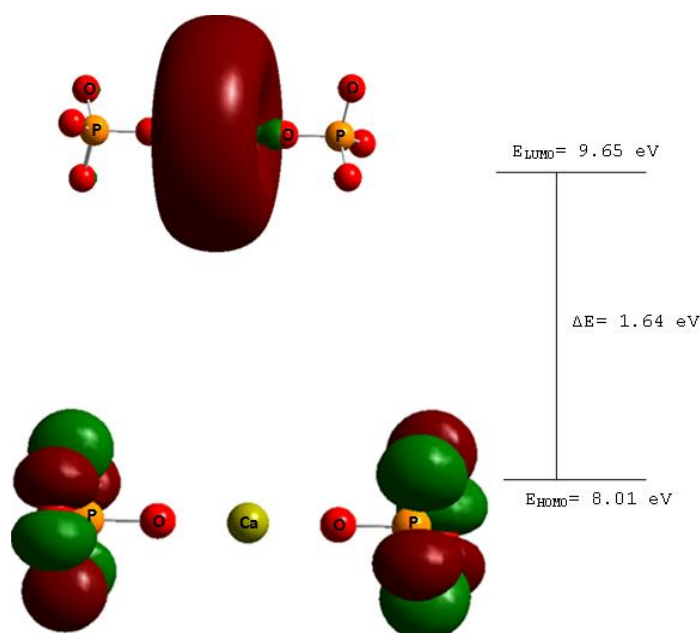

Figure 4. The atomic orbital compositions of the calcium compound by B3LYP/Gen level

TD-DFT calculations were performed on title compund by using the B3LYP/GEN basis set (we used for phosphorus and oxygen 6-31++G(d,p), for calcium cc-pVDZ). The geometry of the singlet ground and excited states were optimized in the gas phase. From these calculations the absorption bands are calculated at 4046.55, 4045.22, 1839.70nm; absorption energies are 0.3064eV, 0.3064eV and 0.6739eV, respectively.

4.3. Molecular Electrostatic Potential
The molecular electrostatic potential has been used to foretell the reactive sides of the molecule and hydrogen bonding interactions as well as their potential use in biological recognition studies [49 ve 50]. MEP was modeled at the B3LYP/Gen level to predict reactive sites and hydrogen bonding interactions. As can easily be seen in Figure 5, the potential changes from -0.47 a.u. to +0.474 a.u..
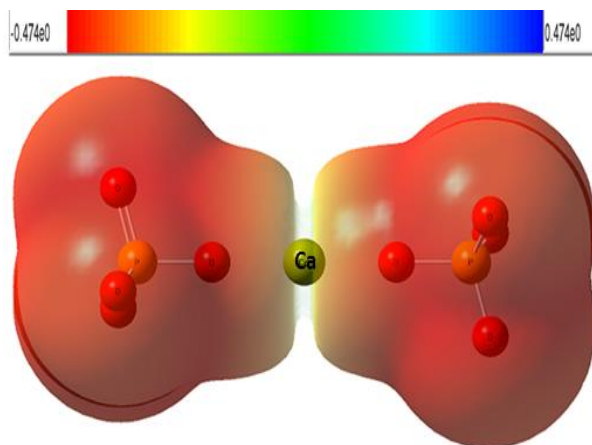

Figure 5. Molecular electrostatic potential (MEP) surface of calcium compound calculated at B3LYP/Gen level

The nano-HAp molecule has two possible sides for nucleophilic attack. The molecule has no positive region while the most of the molecule has negative regions; otherside the molecule has same behavior oppositly. The negative regions are mainly over PO_4 protons. These negative red colored regions represent where the molecule can interact with another molecule or a group.

4.4. NBO Analysis
The efficient method to study intra and intermolecular bonding and charge transfer or conjugative interaction in molecular systems is the NBO analysis [51]. In the NBO analysis the second order Fock matrix was performed to evaluate the donor-acceptor interactions [52]. For each donor and acceptor (j), the stabilization energy $E^{(2)}$ associated with the delocalization i→j is estimated as,

$$E^{(2)} = \Delta E_{ij} = q_i \left[F(i,j)^2 / (\varepsilon_j - \acute{\varepsilon}_i) \right]$$

where q_i is the donor orbital occupancy, are e_j and e_i diagonal elements and $F(i,j)$ is the off diagonal NBO Fock matrix element [53-54]. The larger the $E^{(2)}$ value, the more intensive is the interaction between electron donors and electron acceptors, i.e. the more donating inclination from electron donors to electron acceptors and the greater the extent of conjugation of the whole system. The hyperconjugative interaction energy was derived from the second-order perturbation approach [55 and 56].

Table 4. Second-order perturbation theory analysis of Fock matrix in
NBO Basis for the calcium compound

Donor (i)	ED (i)(e)	Type	Acceptor (j)	Type	ED (j)(e)	E$^{(2)}$ (kJ/mol)	E(j)-E(i) (a.u)	F(i,j) (a.u)
P1-O2	1.96937	σ	P1-O3	σ*	0.16013	10.38	0.87	0.043
			P1-O4	σ*	0.16013	10.38	0.87	0.043
P1-O3	1.96937	σ	P1-O2	σ*	0.16013	10.38	0.87	0.043
			P1-O4	σ*	0.16013	10.38	0.87	0.043
			P1-O7	σ*	0.12570	5.95	1.15	0.037
P1-O4	1.96937	σ	P1-O7	σ*	0.12570	5.95	1.15	0.037
			Ca5-O7	σ*	0.01608	2.55	0.61	0.017
Ca5-O7	1.90107	σ	P1-O2	σ*	0.16013	20.26	0.62	0.049
			P1-O3	σ*	0.16013	19.93	0.62	0.049
			P1-O4	σ*	0.16013	80.39	0.62	0.099
Ca5-O7	1.90107	π	P1-O2	σ*	0.16013	60.12	0.62	0.085
			P1-O3	σ*	0.16013	60.46	0.62	0.085
Ca5-O8	1.90107	σ	P6-O9	σ*	0.16013	19.93	0.62	0.085
			P6-O10	σ*	0.16013	80.39	0.62	0.049
			P6-O11	σ*	0.16013	20.26	0.62	0.049
Ca5-O8	1.90107	π	P6-O9	σ*	0.16013	60.46	0.62	0.085
			P6-O11	σ*	0.16013	60.13	0.62	0.085
P6-O8	1.99174	σ	P6-O10	σ*	0.16013	6.74	1.46	0.045
P6-O9	1.96937	σ	P6-O8	σ*	0.12570	5.95	1.15	0.037
			P6-O10	σ*	0.16013	10.38	0.87	0.043
			P6-O11	σ*	0.16013	10.38	0.87	0.043
P6-O10	1.96937	σ	Ca5-O8	σ*	0.01609	2.55	0.61	0.017
			P6-O8	σ*	0.12570	5.95	1.15	0.017
			P6-O9	σ*	0.16013	10.38	0.87	0.043
			P6-O10	σ*	0.16013	4.438	0.87	0.028
			P6-O11	σ*	0.16013	10.38	0.87	0.043
P6-O11	1.96937	σ	P6-O8	σ*	0.12570	5.95	1.15	0.037
			P6-O9	σ*	0.16013	10.38	0.87	0.043
			P6-O10	σ*	0.16013	10.38	0.87	0.043
O3	1.91657	LP2	P1-O2	σ*	0.16013	11.36	0.46	0.032
			P1-O4	σ*	0.16013	11.43	0.46	0.032
			P6-O10	σ*	0.16013	38.73	0.75	0.075
O4	1.91659	LP2	P1-O2	σ*	0.16013	11.39	0.46	0.032
			P1-O3	σ*	0.16013	11.39	0.46	0.032
O7	1.94050	LP1	Ca5	LP1*	0.07109	72.77	0.89	0.011
			Ca5	LP2*	0.03360	32.28	0.81	0.071
			Ca5	LP3*	0.02354	3.22	0.61	0.019
O8	1.94050	LP1	Ca5	LP1*	0.07109	72.77	0.89	0.011
		LP1	Ca5	LP2*	0.03360	32.28	0.81	0.071
			Ca5	LP3*	0.02354	3.23	0.61	0.019
O9	1.91657	LP2	P1-O7	σ*	0.12570	38.73	0.75	0.075
			P6-O8	σ*	0.12570	38.73	0.75	0.075
			P6-O10	σ*	0.16013	11.43	0.46	0.032
			P6-O11	σ*	0.16013	11.35	0.46	0.032

The NBO analysis point out remarkable donor-acceptor type
delocalization from lone-pair (LP) of oxygen orbitals with anti-lone-
pair (LP*) of metal orbital. The delocalization effects because of the
LP-LP* interactions in title compound play an extremely significant
role on the coordination environments of the Ca^{+2} ion. The
hyperconjugative σ→σ* interactions represent the weak departures from
a strictly localized natural Lewis structure that compose the primary
"noncovalent" effects [57]. As seen from the Table 4, the strongest
stabilization energy calculated as 72.77 kcal/mol between LP(1) O7 and
LP*(1) Ca5 and LP(1) O8 and LP*(1) Ca5. The interactions between
σ(Ca5-O7)→σ*(P1-O4) has 80.39 kcal/mol, σ(Ca5-O7)→σ*(P6-O10) has 80.39
kcal/mol, π(Ca5-O7)→σ*(P1-O2) has 60.12 kcal/mol, π(Ca5-O7)→σ*(P1-O3)

has 60.46 kcal/mol, π(Ca5-O8)$\rightarrow\sigma^*$(P6-O9) has 60.12 kcal/mol, and π(Ca5-O8)$\rightarrow\sigma^*$(P6-O11) has 60.13 kcal/mol give the structure a strong stabilization. The orbital overlap between bonding (π) and anti-bonding (σ^*) orbitals caused the charge transfer interactions bring about the stabilization of the system.

5. CONCLUSION (SONUÇ)

A classical interatomic force field for calcium compound $Ca(PO_4^-)_2$ compound has been derived from density functional theory calculations based on a hybrid B3LYP Hamiltonian and 6-31++G(d,p) basis set of double-zeta polarized quality. The scope of such a derivation is to apply it in further computationally demanding studies related to the comprehension of the geometric, spectroscopic and electronic features of the nano-HAp. The results of study show that studied of title compound is relatively similar with the nano hydroxyapatite and also can applied to a variety of biomolecules related hydroxyapatite without apatite parts and can enhance our understanding biomaterials nature and behavior used in many areas.

REFERENCES

1. Young, R.A. and Brown, W.E., (1982). Biological Mineralization and Demineralization. New York: Springer Verlag.
2. Huang, Y., Wang, H., and Gong, S., (2012). Sorption Behavior of Hydroxyapatite for 109Cd(II) as a Function of Environmental Conditions. Journal of Radioanalytical and Nuclear Chemistry, 292(2), 545-553. http://doi.org/10.1007/s10967-011-1439-6.
3. Gok, C., (2014). Neodymium and Samarium Recovery by Magnetic Nano-Hydroxyapatite. Journal of Radioanalytical and Nuclear Chemistry, 301(3), 641-651. http://doi.org/10.1007/s10967-014-3193-z.
4. Hou, R., Zhang, G., Du, G., Zhan, D., Cong, Y., Cheng, Y., and Fu, J., (2013). Magnetic Nanohydroxyapatite/Pva Composite Hydrogels for Promoted Osteoblast Adhesion and Proliferation. Colloids and Surfaces B: Biointerfaces, 103, 318-325. http://doi.org/10.1016/j.colsurfb.2012.10.067.
5. Kim, I.S. and Kumta, P.N., (2004). Sol-Gel Synthesis and Characterization of Nanostructured Hydroxyapatite Powder. Materials Science and Engineering: B (Vol. 111).
6. Murugan, R. and Ramakrishna, S., (2005). Crystallographic Study of Hydroxyapatite Bioceramics Derived from Various Sources. Crystal Growth & Design, 5(1), 111-112. http://doi.org/10.1021/cg034227s.
7. Rehman, I. and Bonfield, W., (1997). Characterization of Hydroxyapatite and Carbonated Apatite By Photo Acoustic FTIR Spectroscopy. Journal of Materials Science: Materials in Medicine, 8(1), 1-4. http://doi.org/10.1023/A:1018570213546.
8. Tsuda, H. and Arends, J., (1994). Orientational Micro-Raman Spectroscopy on Hydroxyapatite Single Crystals and Human Enamel

Crystallites. Journal of Dental Research, 73(11), 1703–1710.
http://doi.org/10.1177/00220345940730110501.

9. Cuscó, R., Guitián, F., Aza, S.D., and Artús, L., (1998).
Differentiation between Hydroxyapatite and B-Tricalcium
Phosphate By Means Of M-Raman Spectroscopy. Journal of the
European Ceramic Society, 18(9), 1301–1305.
http://doi.org/10.1016/S0955-2219(98)00057-0.

10. Qiu, X., Hong, Z., Hu, J., Chen, L., Chen, X., and Jing, X.,
(2005). Hydroxyapatite Surface Modified by l-Lactic Acid and Its
Subsequent Grafting Polymerization of l-Lactide†.

11. Lee, W.T., Dove, M.T., and Salje, E.K.H., (2000). Surface
Relaxations in Hydroxyapatite. Journal of Physics: Condensed
Matter, 12(48), 9829–9841. http://doi.org/10.1088/0953-
8984/12/48/302.

12. De Leeuw, N.H., Narasaraju, T.S.B., Phebe, D.E., Cho, S.B.,
Miyaji, F., Kokubo, T., and Harding, J.H., (2004). A Computer
Modelling Study of The Uptake and Segregation of Fluoride Ions
At The Hydrated Hydroxyapatite (0001) Surface: Introducing A Ca
10(PO 4) 6(OH) 2 Potential Model. Phys. Chem. Chem. Phys., 6(8),
1860–1866. http://doi.org/10.1039/B313242K.

13. Calderín, L., Stott, M.J., and Rubio, A. (2003). Electronic and
Crystallographic Structure of Apatites. Physical Review B,
67(13), 134106. http://doi.org/10.1103/PhysRevB.67.134106.

14. De Leeuw, N.H., Romer, R.L., Menzies, M., Gallagher, K.,
Yelland, A., Hurford, A.J., and Catlow, C.R.A., (2002). Density
Functional Theory Calculations of Local Ordering of Hydroxyl
Groups and Fluoride Ions in Hydroxyapatite. Physical Chemistry
Chemical Physics, 4(15), 3865–3871.
http://doi.org/10.1039/b203114k.

15. Karabacak, M., Şahin, E., Çınar, M., Erol, İ., and Kurt, M.,
(2008). X-Ray, FT-Raman, FT-IR Spectra And Ab Initio HF, DFT
Calculations Of 2-[(5-Methylisoxazol-3-Yl)Amino]-2-Oxo-Ethyl
Methacrylate. Journal of Molecular Structure, 886(1), 148–157.
http://doi.org/10.1016/j.molstruc.2007.11.014.

16. Xuan, X., Wang, J., Zhao, Y., and Zhu, J., (2007). Experimental
and Computational Studies on the Solvation of Lithium
Tetrafluorobrate in Dimethyl Sulfoxide. Journal of Raman
Spectroscopy, 38(7), 865–872. http://doi.org/10.1002/jrs.1732.

17. Karabacak, M., Çoruh, A., and Kurt, M., (2008). FT-IR, FT-Raman,
NMR Spectra, and Molecular Structure Investigation of 2,3-
Dibromo-N-Methylmaleimide: A Combined Experimental and
Theoretical Study. Journal of Molecular Structure, 892(1), 125–
131. http://doi.org/10.1016/j.molstruc.2008.05.014.

18. Sundaraganesan, N., Meganathan, C., Joshua, B.D., Mani, P., and
Jayaprakash, A., (2008). Molecular Structure and Vibrational
Spectra of 3-Chloro-4-Fluoro Benzonitrile by Ab Initio HF and
Density Functional Method. Spectrochimica Acta Part A: Molecular
and Biomolecular Spectroscopy, 71(3), 1134–1139.
http://doi.org/10.1016/j.saa.2008.03.019.

19. Sundaraganesan, N., Anand, B., Meganathan, C., Joshua, B.D.,
(2008). FT-IR, FT-Raman Spectra and Ab Initio HF, DFT
Vibrational Analysis of P-Chlorobenzoic Acid. Spectrochimica
Acta Part A: Molecular and Biomolecular Spectroscopy, 69(3),
871–879. http://doi.org/10.1016/j.saa.2007.05.051.

20. Xuan, X. and Zhai, C., (2011). Quantum chemical studies of FT-IR
and Raman spectra of methyl 2,5-dichlorobenzoate. Spectrochimica
Acta Part A: Molecular and Biomolecular Spectroscopy, 79(5),
1663–1668. http://doi.org/10.1016/j.saa.2011.05.032.

21. Anoop, M.R., Binil, P.S., Suma, S., Sudarsanakumar, M.R., Sheena
    M.Y., Varghege, H.T., and Panicker, C.Y., (2010). Vibrational
    Spectroscopic Studies and Computational Study of Ethyl Methyl
    Ketone Thiosemicarbazone. Journal of Molecular Structure,
    969(1), 48-54. http://doi.org/10.1016/j.molstruc.2010.01.041.
22. Atac, A., Karabacak, M., Karaca, C., Kose, E., (2012). NMR, UV,
    FT-IR, FT-Raman spectra and molecular structure (monomeric and
    dimeric structures) investigation of nicotinic acid N-oxide: A
    combined experimental and theoretical study. Spectrochimica Acta
    Part A: Molecular and Biomolecular Spectroscopy, 85(1), 145-154.
    http://doi.org/10.1016/j.saa.2011.09.048.
23. Karabacak, M., Cinar, Z., Kurt, M., Sudha, S., and
    Sundaraganesan, N., (2012). FT-IR, FT-Raman, NMR and UV-vis
    Spectra, Vibrational Assignments and DFT Calculations of 4-butyl
    Benzoic Acid. Spectrochimica Acta Part A: Molecular and
    Biomolecular Spectroscopy, 85(1), 179-189.
    http://doi.org/10.1016/j.saa.2011.09.058.
24. Nagabalasubramanian, P.B., Karabacak, M., and Periandy, S.,
    (2012). Molecular Structure, Polarizability, Hyperpolarizability
    Analysis and Spectroscopic Characterization of 1-(chloromethyl)-
    2-methylnaphthalene with Experimental (FT-IR and FT-Raman)
    Techniques and Quantum Chemical Calculations. Spectrochimica
    Acta Part A: Molecular and Biomolecular Spectroscopy, 85(1), 43-
    52. http://doi.org/10.1016/j.saa.2011.09.001.
25. Kurt, M., Raci Sertbakan, T., Özduran, M., and Karabacak, M.,
    (2009). Infrared and Raman Spectrum, Molecular Structure and
    Theoretical Calculation of 3,4-dichlorophenylboronic acid.
    Journal of Molecular Structure, 921(1), 178-187.
    http://doi.org/10.1016/j.molstruc.2008.12.048.
26. Chermette, H., (1998). Density Functional Theory: A Powerful
    Tool for Theoretical Studies in Coordination Chemistry.
    Coordination Chemistry Reviews, 178, 699-721.
    http://doi.org/10.1016/S0010-8545(98)00179-9.
27. Frisch, M.J., Trucks, G.W., Schlegel, H.B., Scuseria, G.E.,
    Robb, M.A., Cheeseman, J.R., Scalmani, G., Barone, V.,
    Petersson, G.A., Nakatsuji, H., Li, X., Caricato, M., Marenich,
    A., Bloino, J., Janesko, B.G., Gomperts, R., Mennucci, B.,
    Hratchian, H.P., Ortiz, J.V., Izmaylov, A.F., Sonnenberg, J.L.,
    Williams-Young, D., Ding, F., Lipparini, F., Egidi, F., Goings,
    J., Peng, B., Petrone, A., Henderson, T., Ranasinghe, D.,
    Zakrzewski, V.G., Gao, J., Rega, N., Zheng, G., Liang, W., Hada,
    M., Ehara, M., Toyota, K., Fukuda, R., Hasegawa, J., Ishida, M.,
    Nakajima, T., Honda, Y., Kitao, O., Nakai, H., Vreven, T.,
    Throssell, K., Montgomery, J.A., Peralta, J.E., Ogliaro, F.,
    Bearpark, M., Heyd, J.J., Brothers, E., Kudin, K.N., Staroverov,
    V.N., Keith, T., Kobayashi, R., Normand, J., Raghavachari, K.,
    Rendell, A., Burant, J.C., Iyengar, S.S., Tomasi, J., Cossi, M.,
    Millam, J.M., Klene, M., Adamo, C., Cammi, R., Ochterski, J.W.,
    Martin, R.L., Morokuma, K., Farkas, O., Foresman, J.B., and Fox,
    D.J., (2016). Gaussian 09, Revision C.01. Gaussian, Inc.,
    Wallingford CT.
28. Dennington, J.M.R. and Keith, T., (2009). GaussView, Version 5.
29. Adamo, C. and Barone, V., (1999). Toward Reliable Density
    Functional Methods without Adjustable Parameters: The PBE0
    Model. The Journal of Chemical Physics, 110(13), 6158.
    http://doi.org/10.1063/1.478522.

30. Avcı, D., (2009). Heteroatom Içeren Bazı Aromatik Moleküllerin Lineer Olmayan Optik Ve Spektroskopik Özelliklerinin Teorik Olarak Incelenmesi. Sakarya University.
31. Francl, M.M., Pietro, W.J., Hehre, W.J., Binkley, J.S., Gordon, M.S., DeFrees, D.J., and Pople, J.A., (1982). Self-Consistent Molecular Orbital Methods. XXIII. A Polarization-Type Basis Set For Second-Row Elements. The Journal of Chemical Physics, 77(7), 3654. http://doi.org/10.1063/1.444267
32. Hariharan, P.C. and Pople, J.A., (1973). The Influence of Polarization Functions on Molecular Orbital Hydrogenation Energies. Theoretica Chimica Acta, 28(3), 213-222. http://doi.org/10.1007/BF00533485.
33. Figgen, D., Rauhut, G., Dolg, M., and Stoll, H., (2005). Energy-Consistent Pseudopotentials for Group 11 And 12 Atoms: Adjustment to Multi-Configuration Dirac-Hartree-Fock Data. Chemical Physics, 311(1), 227-244. http://doi.org/10.1016/j.chemphys.2004.10.005.
34. Peterson, K.A. and Puzzarini, C., (2005). Systematically Convergent Basis Sets For Transition Metals. II. Pseudopotential-Based Correlation Consistent Basis Sets For the Group 11 (Cu, Ag, Au) and 12 (Zn, Cd, Hg) Elements. Theoretical Chemistry Accounts, 114(4-5), 283-296. http://doi.org/10.1007/s00214-005-0681-9.
35. Pedone, A., Corno, M., Civalleri, B., Malavasi, Gianluca, Menziani, M.C., Segrea, U., and Ugliengo, P., (2007). An Ab Initio Parameterized Interatomic Force Field For Hydroxyapatite, Journal of Materials Chemistry. http://doi.org/10.1039/b617858h.
36. Hearmon, R.F.S., (1984). The Elastic Constants of Crystals and Other Anisotropic Materials, Springer-Verlag, Berlin.
37. Saenger, A.T. and Kuhs, W.F., (1992). Z. Kristallogr., 199, 123.
38. Zhu, W. and Wu, P., (2004). Surface Energetics of Hydroxyapatite: A DFT Study. Chemical Physics Letters (Vol: 396). http://doi.org/10.1016/j.cplett.2004.08.006.
39. Fiorentini, V. and Methfessel, M., (1996). Extracting Convergent Surface Energies from Slab Calculations. Journal of Physics: Condensed Matter, 8(36), 6525-6529. http://doi.org/10.1088/0953-8984/8/36/005.
40. Abramowitz, M. and Stegun, I.A., (1972). Handbook of Mathematical Functions. New York: Dover Publications.
41. Tsuda, H. and Arends, J., (1994). Orientational Micro-Raman Spectroscopy on Hydroxyapatite Single Crystals and Human Enamel Crystallites. Journal of Dental Research, 73(11), 1703-1710. http://doi.org/10.1177/00220345940730110501.
42. Cuscó, R., Guitián, F., Aza, S.D., and Artús, L., (1998). Differentiation between Hydroxyapatite and B-Tricalcium Phosphate By Means Of M-Raman Spectroscopy. J. Eur. Ceram. Soc. 18(9), 1301-1305.
43. Fukui, K., (1982). Role of Frontier Orbitals in Chemical Reactions. Science (New York, N.Y.), 218(4574), 747-54. http://doi.org/10.1126/science.218.4574.747.
44. Gümüş, H.P., Tamer, Ö., Avcı, D., and Atalay, Y., (2014). Quantum Chemical Calculations on The Geometrical, Conformational, Spectroscopic and Nonlinear Optical Parameters Of 5-(2-Chloroethyl)-2,4-Dichloro-6-Methylpyrimidine. Spectrochimica Acta Part A: Molecular and Biomolecular Spectroscopy, 129, 219-226. http://doi.org/10.1016/j.saa.2014.03.031

45. Kurtaran, R., Odabaşıoğlu, S., Azizoglu, A., Kara, H., and Atakol, O., (2007). Experimental And Computational Study On [2,6-Bis(3,5-Dimethyl-N-Pyrazolyl)Pyridine]-(Dithiocyanato)Mercury(II). Polyhedron, 26(17), 5069-5074. http://doi.org/10.1016/j.poly.2007.07.021.

46. Kara, İ., Kara, Y., Öztürk Kiraz, A., and Mammadov, R., (2015). Theoretical Calculations of A Compound Formed by Fe+3 and Tris(Catechol). Spectrochimica Acta Part A: Molecular and Biomolecular Spectroscopy, 149, 592-599. http://doi.org/10.1016/j.saa.2015.04.058.

47. Castro, A., Marques, M.A.L., Varsano, D., Sottile, F., and Rubio, A., (2009). The Challenge of Predicting Optical Properties of Biomolecules: What Can We Learn From Time-Dependent Density-Functional Theory? Comptes Rendus Physique, 10(6), 469-490. http://doi.org/10.1016/j.crhy.2008.09.001.

48. Gang, Z. and Musgrave, C.B., (2007). Comparison of DFT Methods for Molecular Murray, J.S. (Jane S., Sen, K.D. (Kali, D., (1996). Molecular Electrostatic Potentials : Concepts and Applications. Elsevier. Orbital Eigenvalue Calculations.

49. Murray, J.S., (Jane, S. and Sen, K.D.,)(1996). Molecular Electrostatic Potentials : Concepts and Applications. Elsevier.

50. Scrocco, E. and Tomasi, J., (1978). Electronic Molecular Structure, Reactivity and Intermolecular Forces: An Euristic Interpretation by Means of Electrostatic Molecular Potentials. Advances in Quantum Chemistry, 11, 115-193. http://doi.org/10.1016/S0065-3276(08)60236.

51. Tomasi, J., Mennucci, B., and Cammi, R., (2005). Quantum Mechanical Continuum Solvation Models.

52. Snehalatha, M., Ravikumar, C., Hubert Joe, I., Sekar, N., and Jayakumar, V.S., (2009). Spectroscopic Analysis and DFT Calculations of A Food Additive Carmoisine. Spectrochimica Acta Part A: Molecular and Biomolecular Spectroscopy, 72(3), 654-662. http://doi.org/10.1016/j.saa.2008.11.017.

53. Szafran, M., Komasa, A., and Bartoszak-Adamska, E., (2007). Crystal and Molecular Structure Of 4-Carboxypiperidinium Chloride (4-Piperidinecarboxylic Acid Hydrochloride). Journal of Molecular Structure, 827(1), 101-107. http://doi.org/10.1016/j.molstruc.2006.05.012.

54. Schwenke, D.W. and Truhlar, D.G., (1985). Systematic Study of Basis Set Superposition Errors in the Calculated Interaction Energy of Two HF Molecules. The Journal of Chemical Physics, 82(5), 2418. http://doi.org/10.1063/1.448335.

55. Reed, A.E. and Weinhold, F., (1983). Natural Bond Orbital Analysis of Near-Hartree-Fock Water Dimer. The Journal of Chemical Physics, 78(6), 4066-4073. http://doi.org/10.1063/1.445134.

56. Foster, J.P., and Weinhold, F., (2002). Natural Hybrid Orbitals.

57. Dege, N., Şenyüz, N., Batı, H., Günay, N., Avcı, D., Tamer, Ö., and Atalay, Y., (2014). The Synthesis, Characterization And Theoretical Study On Nicotinic Acid [1-(2,3-Dihydroxyphenyl)Methylidene] Hydrazide. Spectrochimica Acta Part A: Molecular and Biomolecular Spectroscopy, 120, 323-331. http://doi.org/10.1016/j.saa.2013.10.030.